Direct, Real-Time Measurement of Rapid Inorganic Phosphate Release Using a Novel Fluorescent Probe and Its Application to Actomyosin Subfragment 1 ATPase†

Martin Brune, Jackie L. Hunter, John E. T. Corrie, and Martin R. Webb*

National Institute for Medical Research, Mill Hill, London NW7 1AA, U.K.

Received January 25, 1994; Revised Manuscript Received May 4, 1994®

ABSTRACT: A probe has been developed that can rapidly measure micromolar concentrations of inorganic phosphate (P_i), in particular to follow the release of P_i in real time from enzymes such as phosphatases. Its application is described to investigate the mechanism of actomyosin subfragment 1 ATPase. The probe uses the A197C mutant of *Escherichia coli* phosphate binding protein (PBP), generated by oligonucleotide-directed mutagenesis. A new fluorophore, *N*-[2-(1-maleimidyl)ethyl]-7-(diethylamino)coumarin-3-carboxamide (MDCC), was attached to the single cysteine to produce the reporter molecule that was purified free of unlabeled protein and unattached MDCC. The labeled protein has an excitation maximum at 425 nm and emission maximum at 474 nm in the absence of P_i, shifting to 464 nm with a 5.2-fold increase in fluorescence ($\lambda_{max}/\lambda_{max}$) when complexed with P_i at pH 7.0, low ionic strength, 22 °C. The fluorescence increase is not much altered by change to pH 8 or by increase in ionic strength to 1 M. P_i binds tightly ($K_d \sim 0.1$ μM) and rapidly (1.36×10^8 M^{-1} s^{-1}) and the dissociation rate constant is 21 s^{-1}, at pH 7.0, low ionic strength, 22 °C. A variety of phosphate esters were tested to investigate the specificity of the MDCC-PBP and none gave a significant fluorescence increase at 100 μM or higher concentration. ATP weakly inhibited the P_i-induced fluorescence change, indicating that it binds at least 3000-fold weaker than P_i. Because P_i is a widespread contaminant, the probe is used in conjunction with a "P_i mop", consisting of 7-methylguanosine and purine nucleoside phosphorylase, to remove free P_i from solutions by its conversion to ribose 1-phosphate. Because the equilibrium constant of this reaction is >100, free P_i can be reduced below 0.1 μM. The probe was used to measure the rate of P_i release during a single turnover of ATP hydrolysis with actomyosin subfragment 1 from rabbit skeletal muscle, to determine to what extent P_i release contributes to the rate limitation of this ATPase. Using a stopped-flow apparatus, a small lag prior to rapid P_i release was detected at pH 7.0, low ionic strength, between 5 and 22 °C at both high and low [ATP]. For measurements of a single turnover at low [ATP], the observed rate increased with [actin], showing saturation with a K_m with respect to actin of 26 μM. The data at 22 °C and at [actin] that is close to saturating (45–50 μM) fitted a kinetic scheme, comparable with that obtained from other workers, with the following rate constants: ATP binding, $k_{+1} = 6 \times 10^6$ M^{-1} s^{-1}, $k_{-1} = 7$ s^{-1}; ATP cleavage, $k_{+2} = 30$ s^{-1}, $k_{-2} = 15$ s^{-1}; P_i release, $k_{+3} = 45$ s^{-1}, $k_{-3} = 0$ s^{-1}; ADP release, fast.

Inorganic phosphate (P_i) is a ubiquitous constituent of living systems and the ability to monitor rapid P_i changes in real time could be expected to contribute substantially to understanding many biological processes. One such example is the generation of force in muscle fibers via the cyclical interaction of myosin and actin filaments with concomitant ATP hydrolysis. Myosin has cross-bridges that are the site of interaction with actin and the site of ATP hydrolysis. The correlation of the mechanical processes of contraction with elementary steps during ATP hydrolysis is of major importance for understanding the mechanochemical coupling, but direct comparison of these in muscle fibers is difficult. Measurements of several parts of the ATPase cycle have been made (reviewed by Hibberd & Trentham, 1986; Goldman, 1987), and as outlined in reviews, several lines of evidence suggest that release of P_i is closely related to force generation in fibers. Solution studies of actomyosin and their comparison with fibers have been important for understanding the ATP hydrolysis mechanism and this work describes the first direct measurement of P_i release for actomyosin in real time.

In this work, the data will be discussed in terms of the simplified model in Scheme 1 and related to other kinetic measurements. A represents actin, M is myosin subfragment 1, a proteolytic fragment, and steps are numbered such that the forward and reverse rate constants are k_{+i} and k_{-i}, respectively.

For a variety of reasons parts of the ATPase mechanism of actin-activated myosin and its proteolytic fragments remain unclear. Experimental problems include the high viscosity of F-actin, which makes some measurements at high [actin] difficult, and variations in protein preparations and experimental conditions between laboratories, which can markedly affect measurements, for example because interaction of actin and myosin depends greatly on the ionic strength. Furthermore, because there are interactions of two proteins and MgATP, interpretation of data is very model-dependent. Partially inactive proteins can further complicate interpretation. Ligand release steps have been particularly intractible to experimental observation, but it is these parts of the mechanism that require correlation between actomyosin in solution and in fibers, particularly preparations that have been glycerinated or otherwise permeabilized so the medium bathing

† This work was supported by a European Community Twinning Grant, the Human Frontiers Science Program, and the Medical Research Council, U.K.

* Author to whom correspondence should be addressed. Tel: (44)-81-959-3666. Fax: (44)81-906-4477.

® Abstract published in *Advance ACS Abstracts,* June 1, 1994.

0006-2960/94/0433-8262$04.50/0

Scheme 1

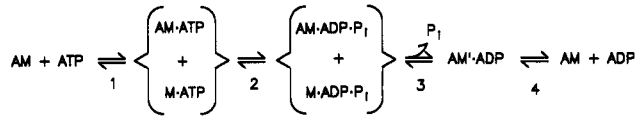

the filaments can be controlled. There has been considerable discussion in the literature about the identity of the rate limiting step and the number of elementary steps in this part of the ATPase mechanism. It is therefore important to have a direct measure of P_i release kinetics that will enable interpretation of this part of the mechanism in terms of the cross-bridge cycle.

Two different types of kinetic experiment that probe the formation and release of P_i for actomyosin in solution and glycerinated fibers will be compared with the direct measurement of P_i release described here. Quenched flow methods have been used to measure the kinetics of P_i formation and hence the presence or absence of a burst formation of bound plus free P_i in the first turnover, more rapid than the steady state (Rosenfeld & Taylor, 1984; Stein et al., 1984; Tesi et al., 1990). The technique requires chemical analysis of the quenched sample to give single time-point information so that several measurements are required to build up a time course of the cleavage. The data give information about the formation of the ADP·P_i state and do not distinguish between bound or unbound P_i. With actomyosin subfragment 1 in solution there has been some controversy as to the presence or size of a burst of P_i formation under some conditions, probably due to the difficulties of getting a complete time course of P_i formation. There is agreement that a burst of P_i formation occurs with myosin in the absence of actin, due to the rapid hydrolysis step followed by slow, rate-limiting P_i release, and that the size of this burst decreases as [actin] increases. However, it seems likely that there is little or no burst for actomyosin subfragment 1 at high [actin] at room temperature or 15 °C, low ionic strength.

Phosphate–water oxygen exchange gives a measure of the rate constant for P_i release, although interpretation is indirect (Bagshaw & Trentham, 1973). Measurements have been done on isolated proteins (Shukla & Levy, 1977; Sleep & Boyer, 1978; Webb & Trentham, 1981; Evans & Eisenberg, 1989; Bowater et al., 1990) and give a measure of the ratio of the rate constants operating on the ADP·P_i complex, k_{+3}/k_{-2} in Scheme 1. Most researchers find little or no exchange during ATP hydrolysis at high [actin], suggesting that P_i release (k_{+3}) is several times faster than the ATP reformation rate constant (k_{-2}).

Myosin or proteolytic subfragment 1 hydrolyzes ATP slowly in the steady state in the absence of actin, and P_i release has been measured in real time (Trentham et al., 1972) and shown to be rate limiting albeit via a slow conformation change of the bound ADP·P_i state (0.04 s^{-1} at pH 8, room temperature). This measurement used a coupled-enzyme method with P_i as substrate for glyceraldehyde phosphate dehydrogenase, although this was not suitable for the much faster rates of actomyosin. More recently a method has been developed using purine nucleoside phosphorylase based on absorbance changes of a nucleoside analogue (Webb, 1992a,b), but is probably not sensitive enough for measurement in single fibers. Several other methods for measuring P_i have been developed on the basis of enzymic reactions (e.g. Lowry & Passonneau, 1972; De Groot & Noll, 1985; Banik & Roy, 1990) that can be coupled to a phosphatase, but none seemed suitable to investigate the actomyosin ATPase in real time both in solution and in fibers.

A new method is described here for measuring P_i release rates that is suitable for fast measurements. This method is based on *Escherichia coli* phosphate binding protein (PBP),[1] the product of the *phoS* gene, which is induced under conditions of P_i starvation and is located in the periplasm as part of the P_i scavenging system of the bacteria. The *phoS* gene has been cloned and sequenced (Magota et al., 1984; Surin et al., 1984) and is expressed with an N-terminal signal sequence that is lost in the mature protein. PBP binds P_i tightly (Medveczky & Rosenberg, 1970), is highly specific (Luecke & Quiocho, 1990) and is a monomeric protein of 35 kDa. The crystal structure for the P_i-bound form has been solved to high resolution and shows two domains with a P_i-binding cleft between them (Luecke & Quiocho, 1990). This class of ligand binding proteins is thought to undergo a large conformation change on ligand binding, with the two domains undergoing a large relative angle change to close the binding cleft (Mao et al., 1982; Sharff et al., 1992) and so it was anticipated that, if PBP was labeled with a fluorophore close to the edge of the cleft, the fluorescent signal might be sensitive to P_i binding. As described below, this hope was realized and the labeled protein was then used as a probe to measure the rate of P_i release from actomyosin subfragment 1 during ATPase activity.

EXPERIMENTAL PROCEDURES

Bacterial Strains and Plasmids. *Escherichia coli* strains TG1 (*supE hsd*Δ5 *thi* Δ(*lac-proAB*), F′[*traD*36 *proAB*$^+$ *lacI*^{q} *lacZ*ΔM15]), and JM109 (*recA*1 *supE*44 *endA*1 *hsdR*17 *gyrA*96 *relA*1 *thi* Δ(*lac-proAB*), F′[*traD*36 *proAB*$^+$ *lacI*^{q} *lacZ* ΔM15]) (Gibson, 1984; Yanisch-Perron et al., 1985) were used for single strand DNA production from phagemid pEMBL9 derivatives (Dente et al., 1983) and for screening of mutated *phoS* genes. *E. coli* strain ANCC75 (*leu purE trp his argG rpsL pho*564 *metA* or *metB thi*) and plasmid pSN5182 containing the *phoS* gene, were provided by Dr. A. Nakata (Osaka University) and were used for overproduction of PBP (Morita et al., 1983).

Materials. LB medium was prepared according to Sambrook et al. (1989). For expression of *phoS*, a minimal medium, TG plus, was used, based on 120 mM Tris·HCl, pH 7.2, containing 80 mM NaCl, 20 mM KCl, 20 mM NH_4Cl, 3 mM Na_2SO_4, 100 mg L^{-1} L-arginine·HCl, 50 mg L^{-1} L-leucine, 40 mg L^{-1} L-histidine·HCl, 20 mg L^{-1} L-methionine, 10 mg L^{-1} L-tryptophan, and 20 mg L^{-1} adenosine.

Because of the need to minimize P_i contamination, precautions were taken with solutions and apparatus used for P_i measurements. Reagents were the highest purity materials available and care was taken with pH meters, which may be contaminated with P_i buffers. Buffers were made at high concentration and diluted prior to use without readjusting the pH. Plasticware was used wherever possible. Prior to use, cuvettes and the stopped-flow apparatus were preincubated with the P_i mop, 7-methylguanosine (typically at 1 mM) and

[1] Abbreviations: PBP, phosphate binding protein; MDCC, *N*-[2-(1-maleimidyl)ethyl]-7-(diethylamino)coumarin-3-carboxamide; MPhCC, *N*-[4-(1-maleimidyl)phenyl]-7-(diethylamino)coumarin-3-carboxamide; MPrCC, *N*-[3-(1-maleimidyl)-1-propyl]-7-(diethylamino)coumarin-3-carboxamide; CPM, 7-(diethylamino)-3-[4′-(1-maleimidyl)phenyl]-4-methylcoumarin; DACM, 7-(dimethylamino)-3-(1-maleimidyl)-4-methylcoumarin; DEM, *N*-[2-(1-maleimidyl)ethyl]-5-(dimethylamino)naphthalenesulfonamide; MIANS, 2-[4′-(1-maleimidyl)anilino]-naphthalene-6-sulfonic acid; MESG, 2-amino-6-mercapto-7-methylpurine ribonucleoside; MDCC-PBP, A197C mutant of PBP labeled with MDCC (other labeled A197C mutants are similarly abbreviated).

purine nucleoside phosphorylase (1 unit mL^{-1}) in the buffer to be used for the measurement.

Myosin subfragment 1 was prepared by chymotryptic digestion of rabbit skeletal myosin as described by Weeds & Taylor (1975) and stored in liquid nitrogen at ~1 mM. Concentrations were calculated on the basis of a molecular weight of 115 000 and $E^{1\%}$(280 nm) = 7.9 cm^{-1}. F-actin from rabbit skeletal muscle was prepared essentially as described by Lehrer and Kerwar (1972). Concentrations were measured from the absorbance spectra assuming $E^{1\%}$(290 nm) $- E^{1\%}$(310 nm) = 6.2 cm^{-1}. Purine nucleoside phosphorylase was the "bacterial" protein from Sigma and was assumed to be one-third active (Webb, 1992a).

Other enzymes were from Boehringer Mannheim, New England Biolabs, and Amersham. Fluorescent labeling reagents were obtained from Molecular Probes (acrylodan, CPM, dansyl aziridine, MIANS) or synthesized (DACM, DEM, MDCC, MPhCC, MPrCC; Corrie, 1990, 1994). All other biochemicals and chemicals were of the highest purity available.

Cloning and Mutagenesis. For site-directed mutagenesis the 1.4 kb EcoR1/Pst1 fragment of pSN5182 containing the *phoS* gene was cloned into the multilinker site of the phagemid vector pEMBL9, yielding pEPS9 (5.4 kb). From this plasmid, ssDNA was prepared according to the method of Dente et al. (1983) using M13K07 as a helper phage. Oligonucleotide-directed site-specific mutagenesis was carried out by the Eckstein phosphorothioate method (Taylor et al., 1985; Nakamaye & Eckstein, 1986). Where applicable, the mutation resulted in a new restriction site such that restriction digests were used for quick identification of mutated *phoS* genes. Mutations were verified by DNA sequencing.

Expression of *phoS* genes from pEPS9 derivatives was low, so the gene was transferred back to pSN5182. The mutated *phoS* genes were excised from pEPS9 as 1.4 kb EcoR1/Pst1 fragments and ligated with the 3.6 kb EcoR1/Pst1 fragment of pSN5182, yielding pSN5182/N plasmids of 5.0 kb. pSN5182/N plasmids were transformed into ANCC75 cells. General cloning techniques were performed as described by Sambrook et al. (1989).

Expression of phoS and Purification of PBP. A 2-mL overnight culture of ANCC75 containing pSN5182 with wild-type or pSN5182/N plasmids with mutated *phoS* genes was diluted into 100 mL of LB medium containing 12.5 mg L^{-1} tetracycline. After 12 h at 37 °C, 10 mL of this culture was diluted into 500 mL of TG plus medium containing in addition 0.64 mM KH_2PO_4, 2 g L^{-1} glucose, 10 μM $FeSO_4$, 0.2 mM $MgSO_4$, 0.2 mM $CaCl_2$, 20 mg L^{-1} tryptophan, 10 mg L^{-1} thiamine and 12.5 mg L^{-1} tetracycline. Cells were grown for 16–20 h, pelleted by centrifugation at 3000 rpm at room temperature for 30 min, and resuspended in 500 mL of TG plus containing the same supplements except 64 μM KH_2PO_4 was used. Cells were grown for another 12–16 h and then harvested.

PBP was released from the cells' periplasm by osmotic shock (Willsky & Malamy, 1976). The final periplasmic extract was buffered with 10 mM Tris·HCl, pH 7.6 and typically had a volume of 40 mL/L of cell culture. The extract was applied to a DEAE-cellulose column (2.6 × 28 cm), equilibrated with 10 mM Tris·HCl, pH 7.6, 1 mM $MgCl_2$. After loading, the column was washed with 1 volume of equilibration buffer, and then a 250-mL continuous gradient of 0–100 mM NaCl in the same buffer was applied. PBP was the major protein present and was pooled and concentrated in an Amicon pressure concentrator. The final protein solution in small aliquots was stored at −80 °C. Protein concentrations were based on absorbance at 280 nm assuming an extinction coefficient ($E^{1\%}$ at 280 nm) of 17.8 cm^{-1}, based on the theoretical value (Gill & von Hippel, 1989) and comparison with a protein assay, using bovine serum albumin as standard (Bradford, 1976).

For binding measurements, the wild-type protein was purified further. The protein was loaded onto a 10-mL Q Sepharose column, equilibrated with 10 mM Tris·HCl, pH 7.6, 1 mM $MgCl_2$. After washing, the protein was eluted by a 200-mL gradient of 0–50 mM NaCl in this buffer. In order to improve the yield of labeled A197C protein in later experiments, this unlabeled mutant protein was loaded onto a 25-mL Q Sepharose column, equilibrated with 10 mM Tris·HCl, pH 7.6, 1 mM $MgCl_2$. After washing, the protein was eluted by a 400-mL gradient of 0–50 mM NaCl in this buffer to give one protein peak.

Labeling A197C PBP with N-[2-(1-Maleimidyl)ethyl]-7-(diethylamino)coumarin-3-carboxamide (MDCC). A197C (100 μM) and MDCC (500 μM, from a 25 mM solution in dimethylformamide) were incubated in 8 mL of 20 mM Tris·HCl, pH 8.1, at room temperature for 4 h on an end-over-end mixer because of a tendency for MDCC to precipitate. The protein was filtered through a 0.2-μm pore size membrane filter (Acrodisc 13, Gelman) and purified on a Biogel P4 gel filtration column (1.5 × 70 cm) eluting with 10 mM Tris·HCl, pH 8.0. The protein was then purified on Q Sepharose as described above for unlabeled mutant, to give two protein peaks, the labeled protein followed by unlabeled, as monitored by absorbance at 280 and 430 nm. The purity of the labeled protein was checked by its fluorescence change with P_i as outlined in the Results section, by its absorbance spectrum, and by SDS gel electrophoresis with both Coomassie Blue staining and fluorescence visualization to observe any non-covalently bound fluorophore. The yield was typically 50% of the starting material for mutant that had not had the extra purification on Q Sepharose prior to labeling and 90% for Q Sepharose purified mutant. The concentration of the labeled protein was determined by the absorbance at 280 nm, after correcting for the absorbance at this wavelength due to the label (0.164 of that at 430 nm). The absorbance spectrum of MDCC attached to PBP was assumed to be the same as that determined for the adduct with dithiothreitol, which had λ_{max} (264 nm) with ϵ 12 800 M^{-1} cm^{-1} and λ_{max} (430 nm) with ϵ 46 800 M^{-1} cm^{-1}. In some preparations the final product contained substoichiometric P_i, but this was variable and could be removed by the P_i mop as described in the Results section.

Other fluorescent labels were attached similarly to PBP mutants, with minor modifications to the procedure, such as the ratio of label to the protein, reaction time, and pH.

Measurements. Absorbance spectra were obtained on a Beckman DU70 spectrophotometer. Fluorescence measurements were obtained on a Farrand Mk1 with xenon lamp and were uncorrected for lamp intensity. Stopped flow experiments were carried out in a HiTech SF61MX apparatus, with a mercury lamp and HiTech IS-2 software. There was a monochromator on the exciting light and a 455-nm cutoff filter on the emission.

The K^+-ATPase of subfragment 1 was measured using the spectrophotometric method of Webb (1992a) based on the release of P_i and also by a pH stat assay based on the release of a proton for each ATP hydrolyzed. For P_i release, the solution contained 50 mM Tris·HCl pH 7.6, 0.6 M KCl, 5 mM EDTA, 5 mM ATP, 200 μM MESG and 12.5 units mL^{-1}

Table 1: Fluorescent Group Labeling of PBP Mutants: Percent Increase in Fluorescence on Adding P_i[a]

	% increase					
fluorophore	A9C	A57C	S139C	G140C	A197C	D292C
acrylodan	10	−3	−15	0	0	19
MDCC	nd	nd	0[c]	nd	405[c]	−2
CPM	15	−4	0[c]	−10	65[c]	−6
DACM	nd	nd	−10	nd	34[c]	0
dansyl aziridine	20	nd	[b]	0	[b]	4
DEM	0	nd	0	0	[b]	nd
MIANS	nd	nd	nd	nd	20	21[d]

[a] The conditions for measurement of fluorescence were ~5 μM labeled PBP in 10 mM Tris·HCl, pH 8.0, to which 50 μM P_i was added. Excitation and emission were at the maximum wavelength. Amino acids are numbered from the N-terminus of the mature protein. nd, not determined. [b] Insufficient labeling to make measurement. [c] Labeled protein was purified on Q Sepharose as described in the Experimental procedures. [d] Using the P_i mop, the fluorescence change was 65%.

purine nucleoside phosphorylase. The absorbance was followed at 360 nm and the reaction was initiated by addition of ~50 nM subfragment 1. For proton release, the solution contained 0.6 M KCl, 5 mM ATP, and 10 mM EDTA at pH 8.0 and 5 mM KOH was titrated to maintain this pH.

The fluorescence titrations of P_i with MDCC-PBP were fitted to the following equations using Enzfitter or Grafit software (Leatherbarrow, 1992) to obtain the dissociation constant, K_d.

Ratio of fluorescence at a given $[P_i]$ to that at zero P_i = $(Q[E_P] + [E] - [E_P])/[E]$, where

$$[E_P] = \frac{[P_i] + [E] + K_d - [([P_i] + [E] + K_d)^2 - 4[P_i][E]]^{1/2}}{2} = [\text{MDCC-PBP}\cdot P_i]$$

and $[P_i]$ = [total P_i], [E] = [total MDCC-PBP], and Q = ratio of fluorescence for MDCC-PBP·P_i to that for the unliganded MDCC-PBP.

RESULTS

PBP was purified from the periplasm of *E. coli* strain ANCC75, overexpressing *phoS* in a multicopy plasmid (Morita et al., 1983). A 4-L culture gave 400–600 mg of PBP with a purity greater than 95% by polyacrylamide gel electrophoresis. The wild-type protein contains no cysteines and so fluorescent groups were attached initially via amines or carboxyls. All attempts to label the wild-type protein with a fluorophore gave at best a 15% fluorescence change on P_i binding, about the same as that observed for the intrinsic tryptophan fluorescence. This is possibly due to relatively nonspecific and multiple labeling. To ensure that a single label could be attached, mutant PBP proteins were obtained by replacing single residues by cysteine, using oligonucleotide-directed mutagenesis. The positions were chosen such that the residues were at the edge of the P_i-binding cleft described by Luecke & Quiocho (1990). These would be expected to experience a significant change in environment on P_i binding, although the structure is known only for the P_i-bound form of PBP. In addition, the mutated residues were not directly involved in P_i binding, as elucidated by Luecke & Quiocho (1990). The cysteine mutants were labeled with a variety of fluorophores and these data are summarized in Table 1. One combination of mutant (A197C) and fluorophore (MDCC; Figure 1) gave a large fluorescence change with P_i, although several closely related fluorophores, including CPM and

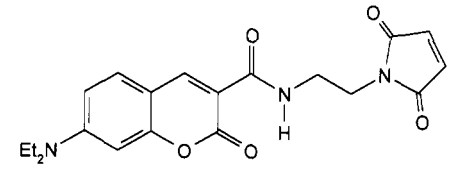

FIGURE 1: Structure of MDCC.

DACM, gave much smaller changes. Two probes, MPhCC and MPrCC, differing from MDCC in only the linker between protein and fluorophore, gave small negative changes with P_i (−22% and −4%, respectively) when bound to the A197C mutant. The MDCC-labeled A197C mutant protein gave by far the largest signal with P_i and was chosen for further study. Most other labeled mutants were not tested to determine whether the lack of P_i sensitivity is because they lacked P_i binding or because the fluorophore is insensitive to the putative conformational change. Serine 139 is involved in P_i binding (Luecke & Quiocho, 1990), so the labeled S139C mutant PBP might be expected to be deficient in P_i binding: this labeled mutant was therefore prepared and used as a null control. The A197C mutant was overproduced to the same extent as wild-type protein, so large amounts of the labeled protein could be obtained.

The yield of P_i-sensitive labeled mutant, MDCC-PBP, was considerably higher after the unlabeled protein had undergone Q Sepharose purification as described in the Experimental Procedures, rather than after the single DEAE-cellulose column. This probably relates to removing P_i, as labeling is very poor in the presence of added P_i. MDCC-PBP was purified further and tested as described in the Experimental Procedures to show it was a singly-labeled protein with no unlabeled protein or free fluorophore. This further purification is important as the unlabeled protein will also bind P_i. Unbound fluorophore would reduce the percentage fluorescence change by increasing the background and it might also slowly react with or bind to other components in the experimental system. Ion-exchange chromatography separated MDCC-PBP completely from unlabeled PBP and unbound fluorophore, as shown by the ratio of absorbance 280/430 nm, with the final labeled protein having a ratio of 1.6.

The fluorescence excitation maximum is 425 nm and the emission maximum is 474 nm in the absence of P_i. With excess P_i at pH 7.0 for the conditions in Figure 2, there is a shift of maximum emission to 464 nm and the fluorescence increases 5.2-fold ($\lambda_{max}/\lambda_{max}$). The labeled protein could be stored at −80 °C and was stable on ice for at least 5 days. The final product contained a variable amount of P_i that was typically less than 20% (mol/mol) of the active protein.

The P_i-dependent fluorescence change of MDCC-PBP was measured for a variety of conditions at a single concentration of P_i, in order to test its suitability for use in the range of pH 7–8 or at high ionic strength. The 5.2-fold fluorescence increase in 10 mM PIPES, pH 7.0 reduced to 5.1 in 10 mM Tris·HCl (pH 8.0) and to 4.5 in 20 mM PIPES (pH 7.0), 1 M NaCl.

Equilibrium Interactions of MDCC-PBP with P_i. When P_i was titrated into 5 μM MDCC-PBP, the fluorescence responded linearly to P_i up to 0.75–0.80 molar ratio of P_i to protein (Figure 3). Beyond that ratio, there is little further fluorescence increase, suggesting that the protein is 75–80% active, with the remaining protein binding P_i weakly if at all. The basis of this inactive portion is not yet understood.

The dissociation constant was determined by titrating P_i at low [MDCC-PBP] and measuring fluorescence (Figure 4).

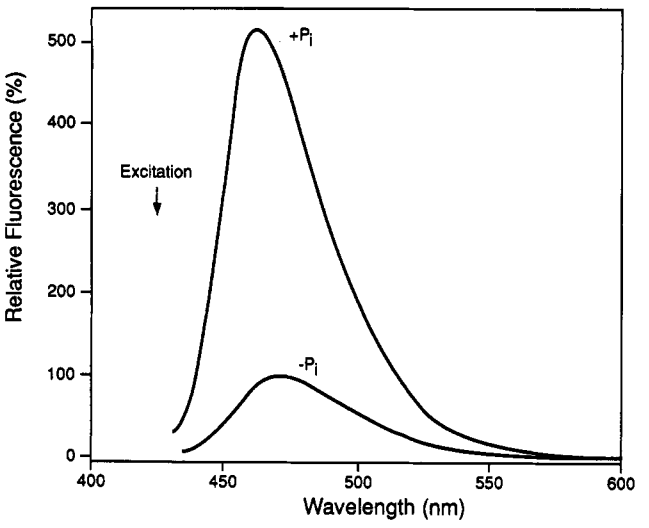

FIGURE 2: Fluorescence emission spectra of MDCC-PBP in the presence and absence of P_i. 3.2 μM MDCC-PBP was in 10 mM PIPES, 1 mM $MgCl_2$ (pH 7.0) at 22 °C. P_i was added to 50 μM.

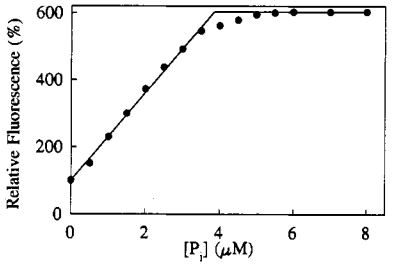

FIGURE 3: Correlation between the fluorescence increase and [P_i] added to the MDCC-PBP. The solution at 20 °C contained 5 μM MDCC-PBP, 1 mM $MgCl_2$, 10 mM PIPES, pH 7.0. Aliquots of P_i were added and the fluorescence emission was measured at 465 nm with excitation at 425 nm. The data were corrected for the small amount of dilution.

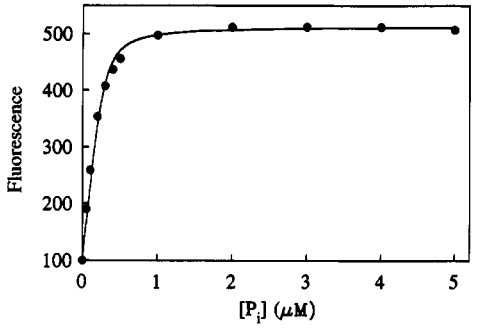

FIGURE 4: Titration of P_i to MDCC-PBP to obtain the dissociation constant. The solution at 25 °C in 10 mM PIPES, pH 7.0, 1 mM $MgCl_2$ contained 0.28 μM MDCC-PBP. Aliquots of P_i were added, and the fluorescence emission was measured as in Figure 3. The data fit a simple binding model and the line shows the best fit K_d = 0.03 μM, although all values <0.1 μM fit well. The maximum fluorescence enhancement is 5.15-fold.

This shows that binding is tight, and the curve fits a dissociation constant of 0.03 μM at pH 7.0; a value of 0.08 μM was obtained at pH 8.0. Because these dissociation constants are well below the protein concentrations used, they can be considered only approximate: the fluorescence titration could not be done at sufficiently low concentrations of protein and P_i (because of P_i contamination; see below) to obtain accurate values of K_d.

K_d for Wild-Type PBP. In order to determine to what extent the affinity for P_i was affected by the labeling, a comparison was made with wild-type PBP. The value for the K_d for wild-type in the literature is 1 μM (Medveczky & Rosenberg, 1970; Kubena et al., 1986) and we obtained a similar value using a equivalent radioactive assay with wild-type PBP that had been purified on a single ion-exchange column to homogeneity on the basis of SDS–PAGE. Further purification of the wild-type protein on Q Sepharose gave two populations of protein that ran identically on SDS–PAGE. A competition titration of MDCC-PBP·P_i with the first peak of wild-type PBP showed that the latter bound P_i 2-fold tighter than the labeled mutant. The second peak bound P_i more weakly but variably between batches. However, treatment of this second peak with P_i mop (see below) to remove bound P_i prior to the titration gave wild-type that also bound added P_i tightly. It is likely that this bound P_i in the second peak is the cause of two populations of this wild-type protein: the apoprotein and P_i complex run differently on Q-Sepharose. We are therefore confident that the true K_d of wild-type PBP is ~2-fold lower than that for MDCC-PBP.

P_i Mop to Remove P_i Contamination. Because MDCC-PBP binds P_i tightly, low levels of P_i contamination can affect the observed change on adding P_i. Even in the absence of added phosphate compounds, it can be difficult to reduce P_i contamination below 1 μM, as P_i is a fairly ubiquitous contaminant in buffers as well as biological solutions (for a discussion, see Lowry & Passonneau, 1972). Purine nucleotides inevitably have low concentrations of P_i present due to hydrolysis. Proteins can also be contaminated: for example, actin has bound nucleotide and tests showed levels of P_i approximately equimolar with the protein. P_i is also a contaminant that binds to and washes off glassware. While some contaminants can be removed physically, such as by chromatography, it is not feasible to do this completely or simply. Because the P_i probe is not enzymic, once all sites on the MDCC-PBP are bound by P_i, additional P_i does not give a further signal. We therefore made use of a "phosphate mop", an enzymic backup system to remove P_i, that consisted of purine nucleoside phosphorylase with 7-methylguanosine which had previously been shown to be a substrate (Kulikowska et al., 1986). This reaction was characterized as described for the thio analogue MESG (Webb, 1992a). Using the absorbance change at 260 nm to monitor the rate of phosphorolysis, the K_m is 59 μM for 7-methylguanosine and 34 μM for P_i, and k_{cat} = 109 s^{-1} (pH 8.0, 20 mM Tris·HCl, 1 mM $MgCl_2$, 30 °C). The phosphorolysis is essentially irreversible (K_{eq} > 100), and P_i reacts chemically to form ribose 1-phosphate so that it is no longer available to bind tightly to PBP: tests showed that P_i could be reduced below ~0.1 μM. For experiments with the PBP, conditions were chosen such that the enzyme was present at low concentrations, insufficient to compete with the MDCC-PBP for the initial binding of P_i released by the actomyosin, or other system, but sufficient to slowly remove P_i. This is illustrated in Figure 5. Additions of P_i show the rapid fluorescence increase on binding to the MDCC-PBP. Subsequently, the P_i is slowly removed from the protein by the enzymic P_i mop and fluorescence returns to baseline. This process can be repeated several times, although there is a slight rise in baseline each time: this may represent a low residual P_i or the effect of ribose 1-phosphate binding weakly to MDCC-PBP.

Affinity of Other Compounds for MDCC-PBP. Although PBP is specific for P_i (Luecke & Quiocho, 1990), it was to be used as a probe in the presence of other phosphate species, such as esters or purine nucleotides and so it was important to know at what levels these might interfere with P_i measurements. Several phosphate compounds were tested for their

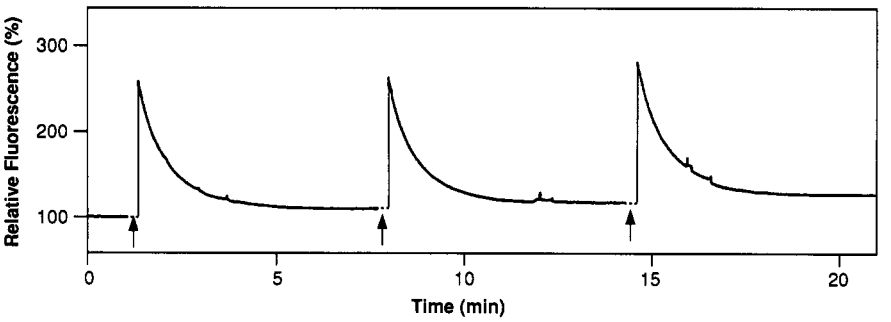

FIGURE 5: Time course of the P_i-induced fluorescence change using the P_i mop to recover unbound MDCC-PBP. The solution contained 10 μM MDCC-PBP, 1 mM 7-methylguanosine and 0.5 unit mL^{-1} purine nucleoside phosphorylase in 10 mM PIPES pH 7.0, 1 mM $MgCl_2$ at 25 °C. Aliquots of P_i (to 5 μM) were added as indicated by the arrows, at time intervals sufficient for the P_i mop to remove P_i from the MDCC-PBP and the fluorescence emission was measured as in Figure 3.

Table 2: Fluorescence Change to MDCC-PBP Due to Potential Inhibitors[a]

additions	% fluorescence increase	additions	% fluorescence increase
P_i (50 μM)	430	glucose 6-phosphate (100 μM)[b]	3
pyrophosphate (100 μM)[b]	6	sodium sulfate (1 mM)	3
ATP (100 μM)[b,c]	2	$BeCl_2$ (100 μM)/NaF (100 mM)	3
ATP (1 mM)[b,c]	11	$AlCl_3$ (100 μM)/NaF (100 mM)	3
GDP (100 μM)[b]	3	sodium arsenate (100 μM)	313
ADP (100 μM)[b]	5	sodium vanadate (100 μM)	35
NPE-caged ATP (5 mM)[b-d]	0		

[a] The solutions contained 2 μM MDCC-PBP in 20 mM PIPES (pH 7.0) at 22 °C except where indicated. The fluorescence change was measured at 465 nm with excitation at 425 nm. After the additions of phosphate compound or analogue, addition of excess P_i induced the full fluorescence increase, except for arsenate (see text). [b] The solution was preincubated with the P_i mop. [c] 10 μM MDCC-PBP. [d] NPE-caged ATP is P^3-1-(2-nitrophenyl)ethyl ATP.

effect on MDCC-PBP fluorescence (Table 2) and none caused a significant increase, after P_i impurities were removed using the P_i mop. Two compounds, caged ATP and ATP, were tested further to find if they inhibited P_i binding significantly by titrating P_i as in Figure 3, but in the presence of the potential inhibitor. Caged ATP (at 5 mM) increased the apparent dissociation constant of P_i to 0.28 μM: ATP (at 1 mM) gave 0.13 μM. These data imply that the affinity of MDCC-PBP for caged ATP or ATP is >3000-fold weaker than P_i.

Several P_i analogues were also tested (Table 2) and only arsenate and vanadate produced significant increases in MDCC-PBP fluorescence. In all cases except arsenate, when subsequently excess P_i was added, the full fluorescent change was observed. A titration of arsenate was done as in Figure 3 to obtain a dissociation constant of 3 μM for arsenate and MDCC-PBP.

Kinetics of P_i Interaction with MDCC-PBP. In order to use the probe to measure P_i release from phosphatases in real time it was important to know the kinetics of P_i interaction with the labeled protein. These were measured in a stopped-flow apparatus and data for P_i binding at pH 7.0 are shown in Figure 6A. Because of the fast rates, only part of the exponential is observed at high [P_i]: a significant proportion of the reaction occurs during the dead time of the instrument (i.e. the time taken for the solution to flow between mixing and observation chambers). The rate constants at [P_i] < 2.5 μM increased linearly with [P_i] (Figure 7), and there is saturation of rates at high [P_i] (data not shown), although it is not clear if this saturation is due to the limitations of the stopped flow instrument or whether there is a two-step binding of P_i, and these data must therefore be treated with caution. The rate of constants at [P_i] < 2.5 μM fitted a simple one-step binding model with the slope of the plot of observed rate constants vs [P_i] being the association rate constant, k_+ = 1.36×10^8 M^{-1} s^{-1} (21 °C, 10 mM PIPES, pH 7.0).

The dissociation rate of the MDCC-PBP·P_i complex was measured in the stopped flow apparatus by mixing this complex with excess wild-type PBP. P_i is released from the fluorescent complex and binds to the wild-type protein with a rate constant limited by the rate of release (Figure 6B). The observed rate was 21.3 ± 0.1 (SEM) s^{-1} (22 °C, 10 mM PIPES, pH 7.0) for wild-type concentrations from 1.25 to 10 μM, with 0.25 μM MDCC-PBP and 0.125 μM P_i. Because this rate is constant over a range of wild-type concentrations and because the rate is much slower than that expected for P_i binding, assuming that the wild-type PBP has similar rate constant to the MDCC-PBP, the observed rate constant probably represents P_i release. Using the value for the rate constants obtained above, $K_d = k_-/k_+ = 0.15$ μM, higher than the value obtained by the titration. At least part of the difference may be due to the presence of low amounts of P_i contamination in the equilibrium titration. Further elaboration of the kinetic mechanism of P_i association is required, but these measurements have shown the range of accessible rates for using MDCC-PBP in assays of P_i release in real time.

CPM-PBP. Some experiments with actomyosin were also done with the A197C mutant protein labeled with CPM. All the methods of characterization described above were also used for CPM-PBP, which has maximum excitation at 397 nm and emission at 478 nm, not much affected by addition of P_i. Titrations with P_i gave a dissociation constant of 14 μM at pH 7.0 and 11 μM at pH 8.0, 2 orders of magnitude weaker than MDCC-PBP. There was a fluorescence enhancement of 2.04-fold at pH 8.0 (10 mM Tris·HCl) and 1.63-fold at pH 7.0 (10 mM PIPES) on adding excess P_i.

Kinetics of P_i Release with Myosin and Actomyosin Subfragment 1. MDCC-PBP was used to measure the kinetics of P_i release from actomyosin subfragment 1 ATPase, to probe the mechanism of this part of the reaction, and to determine to what extent P_i release contributes to rate limitation. The immediate aim was to see if there was any burst of P_i release faster than steady state rate or if P_i release was at the same rate as the steady state rate. For these measurements in the stopped-flow apparatus, [MDCC-PBP] was usually at 9 μM

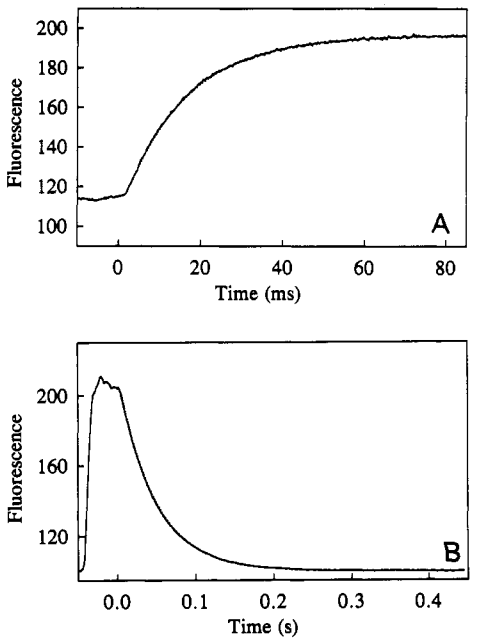

FIGURE 6: Kinetics of P_i binding to MDCC-PBP and its release. (A) 0.1 μM MDCC-PBP (mixing chamber concentration) in 10 mM PIPES, pH 7.0 was mixed at 21 °C with 0.25 μM P_i in this buffer in a stopped-flow apparatus, while fluorescence emission was monitored using a 455 nm cutoff filter, with excitation at 436 nm using a mercury lamp. The signal had a time-averaging filter of <0.1 × half-time. When the flow stops nominally at a time zero, the reaction time course is observed with fluorescence rising as a single exponential. The best fit (65.3 s^{-1}) is shown by the dashed line, almost completely hidden by the experimental curve. The signal before this is due to unreacted solution flowing through the chamber. The initial lag was within the dead time of the apparatus, i.e., the time taken for solution to flow from mixing chamber to observation chamber. (B) The release kinetics were measured by rapidly mixing 0.125 μM P_i, 0.25 μM MDCC-PBP with 10 μM wild-type PBP (mixing chamber concentrations) at 22 °C. Other conditions were as above. In this trace the initial phase is prior to flow starting: the observation chamber contains old solution from the previous reaction, at low fluorescence. The second phase is as flow begins and solution in the mixing chamber is replaced by high fluorescence, unreacted solution. After flow stops, the fluorescence decreases and the best-fit single exponential (21.4 s^{-1}) is shown by the dashed line, almost completely hidden by the experimental curve.

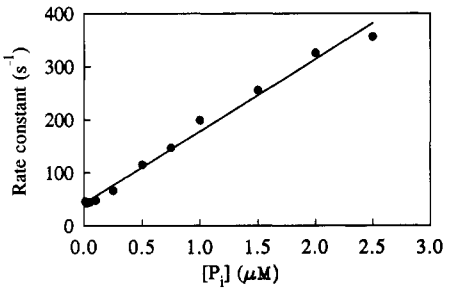

FIGURE 7: The dependence on P_i concentration of the observed rate constant for its association with MDCC-PBP. The rate constants are the best fit exponentials obtained as in Figure 6A. The best fit line has a slope of 1.36×10^8 M^{-1} s^{-1}.

and the components of the P_i mop, 7-methylguanosine and the phosphorylase, were present as outlined above.

An initial experiment measured the rate of P_i release for subfragment 1 in the absence of actin. [ATP] was less than [subfragment 1], so that all the ATP bound and a single turnover of hydrolysis gave rise to P_i release. There was a single exponential increase in fluorescence with a rate constant of 0.09 s^{-1} (pH 7.0, 22 °C) (Figure 8A), consistent with previous measurements (Trentham et al., 1972; Webb, 1992b).

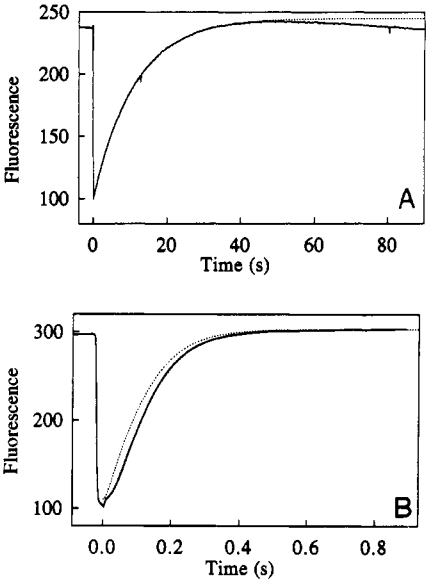

FIGURE 8: The kinetics of P_i release from myosin subfragment 1 and actomyosin subfragment 1 at low [ATP], monitored by MDCC-PBP fluorescence. All solutions in 10 mM PIPES, 1 mM $MgCl_2$, pH 7.0, were mixed in a stopped flow apparatus at 22 °C and monitored as in Figure 6. The following concentrations are those in the mixing chamber. (A) Both syringes contained 100 μM 7-methylguanosine, 0.02 unit mL^{-1} phosphorylase. Solution 1: 8 μM myosin subfragment 1 and 9 μM MDCC-PBP. Solution 2: 2.5 μM ATP. The best fit exponential is also shown, $k = 0.0875$ s^{-1} (almost completely hidden by the experimental line). (B) Solution 1: 9 μM MDCC-PBP, 4 μM subfragment 1, 50 μM 7-methylguanosine, 0.01 unit mL^{-1} phosphorylase. Solution 2: 4 μM ATP, 58 μM actin, 250 μM 7-methylguanosine, 1.5 units mL^{-1} phosphorylase. The P_i release predicted by the model described in the text is shown by the lower dashed line (partially hidden by the experimental line). The upper dashed line shows the theoretical *total* P_i (bound + released) for comparison.

The end of the trace gives a further illustration of the effect of the P_i mop, which slowly reduces the fluorescence by removing P_i. The amount of mop added was selected so that it did not affect the observed rate of fluorescence rise due to the myosin-catalyzed ATP hydrolysis but ensured that the PBP was free of P_i prior to mixing.

Two different types of experiment were done in the presence of actin. In the first [ATP] was similar to [subfragment 1], so that the measurement was essentially of a single turnover, and in the second [ATP] was much higher than [subfragment 1], so that the reaction was multiple turnover. Results of the first type of experiment are shown in Figure 8B, for a measurement at high [actin]. After the flow stopped, there was on most traces an initial, small, rapid increase in fluorescence that had a rate constant expected for free P_i binding to MDCC-PBP (cf. Figure 6A). This usually represented less than 0.3 μM P_i and was probably low residual P_i contamination particularly from actin. The next phase was a lag followed by a rise in fluorescence with a rate that depended on [actin]. The lag was due to early steps in the hydrolysis mechanism as described in the Discussion. The final rise in fluorescence after the lag phase was fitted to a single exponential, and Figure 9 shows the saturation of these fitted exponential rates at high [actin]. The data after the lag phase were fitted to a two-step binding model with step 1 assumed to be much faster than step 2:

$$A + M{\cdot}ADP{\cdot}P_i \rightleftharpoons AM{\cdot}ADP{\cdot}P_i \xrightarrow{k_{+2}} AM{\cdot}ADP + P_i$$

For this, $K_m = 26.0$ μM and $k_{+2} = 15.2$ s^{-1}. Steady-state

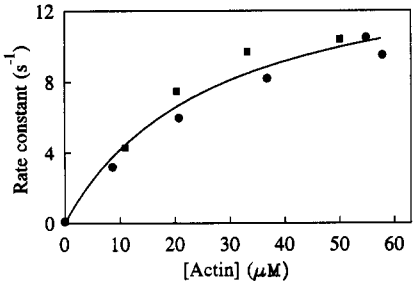

FIGURE 9: Rate of actomyosin subfragment 1 ATPase as a function of actin concentration. The rates are for the best fit exponentials for curves from conditions in Figure 8B: low ATP:subfragment 1 ratio. The best fit curve gives a K_m of 26 μM and maximum exponential rate = 15.2 s^{-1}. The circles and squares represent different sets of measurements with different protein preparations.

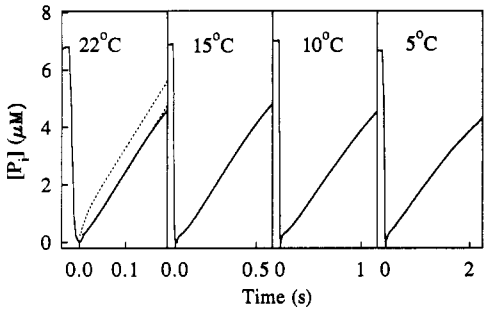

FIGURE 10: The kinetics of P_i release from actomyosin subfragment 1 at high [ATP], monitored by MDCC-PBP fluorescence. The reaction was done at various temperatures as indicated on the traces. All solutions in 10 mM PIPES, 1 mM $MgCl_2$, pH 7.0, were mixed in a stopped flow apparatus and monitored as in Figure 6. The pH of the PIPES buffer was not readjusted at different temperatures. The following concentrations are those in the mixing chamber. For experiments at 22, 15, and 10 °C: Solution 1: 9 μM MDCC-PBP, 2 μM subfragment 1, 50 μM 7-methylguanosine, 0.02 unit mL^{-1} phosphorylase. Solution 2: 100 μM ATP, 45 μM actin, 250 μM 7-methylguanosine, 0.05 unit mL^{-1} phosphorylase. For the experiment at 5 °C, the P_i mop was not so efficient, so both syringes contained 9 μM MDCC-PBP: Solution 1: 2 μM subfragment 1, 50 μM 7-methylguanosine, 0.01 unit mL^{-1} phosphorylase. Solution 2: 100 μM ATP, 45 μM actin, 250 μM 7-methylguanosine, 1.5 units mL^{-1} phosphorylase. The measurement at 10 °C was repeated with these solutions and there was no difference from having PBP in only one syringe. The P_i release at 22 °C predicted by the model described in the text, but assuming an active [subfragment 1] of 1.85 μM, is shown by the lower dashed line (partially hidden by the experimental line). The upper dashed line shows the theoretical *total* [P_i] for comparison.

ATPase measurements gave K_m with respect to actin = 25 μM for similar solution conditions.

To calculate a rate constant (k_{cat}) from steady-state hydrolysis data requires an assumption about the active site concentration of myosin and this makes comparison of single turnover and steady-state data difficult. To get round this problem and to ensure that ATP binding does not contribute to rate limitation, some measurements were done with a large excess of ATP, so that any initial burst of P_i release in the first turnover would be observed before the steady-state P_i release. Experiments were done at 50 or 100 μM ATP, 40–45 μM actin, and 2 or 4 μM subfragment 1 (mixing chamber concentrations) and the results from such an experiment are shown in Figure 10. Because several measurements on P_i formation bursts for actomyosin or fibers have been at lower temperatures (10–15 °C), P_i release kinetics were measured at lower temperatures for comparison (Figure 10). In these experiments there was also a small, initial, rapid burst of fluorescence increase, much less than one turnover of the subfragment 1. Experiments where the data collection was more rapid indicated that the rate was that due to free P_i binding to MDCC-PBP (cf. Figure 6A). Following this there was a lag then a linear rise in fluroescence. The fluorescence rise then slows, which probably represents the onset of MDCC-PBP saturation. The [P_i] scale on these traces is based on the total active [MDCC-PBP] and the total fluorescence change observed when the MDCC-PBP is saturated with P_i.

The slope of the linear phases of these traces showed that the k_{cat} was 14.8 s^{-1} at 22 °C, 4.3 s^{-1} at 15 °C, 2.0 s^{-1} at 10 °C, and 1.0 s^{-1} at 5 °C, assuming fully active subfragment 1. An Arrhenius plot of these rates showed that the k_{cat} has an activation energy of 100 kJ mol^{-1} (SEM 1.6 kJ mol^{-1}). This agrees well with previous data that gave an activation energy of 103 kJ mol^{-1} (Tesi et al., 1991) for the steady-state ATPase at pH 8.0.

DISCUSSION

Characterization of MDCC-PBP. A197C MDCC-PBP shows several properties that are important for its use as a sensitive probe to measure P_i release rates from phosphatases in the pH 7–8 range. It can be prepared as a single molecular species, free of unlabeled protein and unattached fluorophore. MDCC-PBP fluorescence shows a linear response to P_i in the micromolar range and is selective for P_i. It binds P_i rapidly and so is likely to be useful in measuring P_i release rates up to at least 100 s^{-1}. The excitation wavelength (425–436 nm) is higher than the region where most biological molecules absorb.

The data presented here establish the use of this probe for measuring P_i release rates, but there are several features of the PBP that relate to this use that have not been fully elucidated. MDCC-PBP binds P_i tightly, only 2-fold weaker than wild-type PBP. Our value for the wild-type K_d is lower than published values (~1 μM) (Medveczky & Rosenberg, 1970; Kubena et al., 1986) and we think that the weaker binding was due to P_i contamination, which is removed by extra purification by Q Sepharose, with careful exclusion of P_i. Because the kinetics of P_i binding to MDCC-PBP are fast, a significant proportion of the binding reaction at high [P_i] was not observed in the stopped-flow apparatus. We have not yet fully investigated the mechanism of this reaction but have interpreted the data in terms of a single-step binding mechanism. Although the MDCC-PBP is homogeneous by SDS–PAGE and contains no unlabeled protein, it is typically 70–80% active. Some of the inactive protein may be due to P_i contamination, but this is unlikely to account for all the inactive portion. One possibility is some rearrangement of the attached label that prevents P_i binding and possible mechanisms include hydrolysis or aminolysis of maleimides after formation of their thiol adducts (Wu et al., 1976).

During the trial of different fluorophores for P_i sensitivity, several were tested that are related to MDCC, and their lack of sensitivity indicates that precise structural requirements must be met for a probe to be sensitive to the protein conformational change on binding P_i. Similar coumarin fluorophores, DACM which has no spacer, and CPM with a phenylene spacer are much less sensitive to P_i when bound to the same cysteine. The two close analogues of MDCC, MPhCC with a phenylene spacer and MPrCC with a propylene spacer, show a decrease in fluorescence with P_i. Furthermore, CPM-PBP has a 100-fold reduction in affinity for P_i relative to MDCC-PBP.

P_i Mop. A problem when working with small changes in [P_i] in biochemical buffers or biological solutions is contamination by P_i, either from breakdown of phosphate compounds

or from impurities in glassware, buffers, etc. The use of 7-methylguanosine and purine nucleoside phosphorylase as a P_i mop with MDCC-PBP can overcome most of these problems. It removes P_i both from free solution and when bound to PBP, reducing [P_i] to below 0.1 μM. If a low concentration of the phosphorylase is present, it does not compete significantly with the rapid binding of released or added P_i to MDCC-PBP but enables the probe to be free of P_i at the start of the experiment.

P_i Release Kinetics from Actomyosin Subfragment 1. MDCC-PBP has been used to make the first direct measurement of P_i release for actomyosin subfragment 1 ATPase in solution. We have shown that in the first turnover of ATP in solution there is no burst of P_i release, faster than the steady-state ATPase rate (low ionic strength, pH 7.0, 5–22 °C). This provides direct experimental evidence that the rate-limiting step is P_i release or a step preceding it. The data presented here were tested by the model in Scheme 1, to determine to what extent our data fit a set of rate constants consistent with other work and to what extent variations in these rate constants can be accommodated. Figures 8 and 10 show the theoretical curves at 22 °C with high [actin], for the following rate constants: $k_{+1} = 6 \times 10^6$ M^{-1} s^{-1}, $k_{-1} = 7$ s^{-1}, $k_{+2} = 30$ s^{-1}, $k_{-2} = 15$ s^{-1}, $k_{+3} = 45$ s^{-1}, $k_{-3} = 0$ s^{-1}, $k_{+4} = 250$ s^{-1}, $k_{-4} = 0$ s^{-1}. This set of rate constants is compatible with a variety of other measurements, as discussed below. The kinetics of total P_i formation (as opposed to released P_i) predicted by this model are shown as the upper theoretical curves in Figure 8 and 10. This shows a small burst in Figure 10, for which [actin] is high but not saturating, but the model predicts zero burst at saturating [actin]. The lag in the released P_i curves is mainly due to the cleavage step, although there is also a small lag due to ATP binding at low [ATP] (Figure 8), also present in the predicted total P_i curve and absent at high [ATP]. Not surprisingly, the size of the lag at low [ATP] (Figure 8) is predicted to be sensitive to the rate constant for ATP binding, but this sensitivity is lost at high [ATP]. However, in the latter case the observed rate depends on the active myosin concentration, as stated in the Figure 10 legend: information is obtained from the shape of the traces rather than the absolute rates. The extent to which the rate constants can be varied and still fit the P_i release data is discussed below.

There is a range of values suggested in the literature for ATP binding and release rate constants, and comparison is made difficult by differing conditions as outlined in the Introduction. Biosca et al. (1984) estimated limits on ATP release (>5 s^{-1} at 15 °C) based on ATP cold chase measurements. Sleep & Hutton (1980) (2 s^{-1}) and Bowater et al. (1990) (8 s^{-1}) used isotope exchange techniques to estimate this rate constant. The values chosen here are in this range. A variety of ATP dependent signals have been used previously to obtain ATP binding rate constants of $\sim 10^6$–10^7 M^{-1} s^{-1}. The values for the cleavage rate constants are close to those of Rosenfeld and Taylor (1984). The ratio of $k_{+3}/k_{-2} = 3$ is in line with oxygen exchange measurements showing little exchange. It is clear from a number of estimates that ADP release is accelerated over a 100-fold by the presence of actin from the rate of myosin alone (Hibberd & Trentham, 1986). As shown in Figure 10, this set of rate constants predicts a low (<15%) total P_i formation burst prior to the steady-state rate, compatible with the data of Rosenfeld and Taylor (1984) and Tesi et al. (1990).

Although the set of rate constants discussed above gives a good fit to the P_i release data, we considered to what extent the fit is sensitive to altering individual rate constants in this set. The fit is relatively insensitive to changing the rate constants for reverse steps or for ADP release. Changes in one of the other three rate constants by ±20% affect the fit adversely, unless compensating changes are made in the other two rate constants. The model was tested by considering what variations in k_{+2} and k_{+3} can be made without changing other rate constants while maintaining a good fit to the data, to explore to what extent P_i release can limit the overall rate. $k_{+2} = 41$ s^{-1} and $k_{+3} = 30$ s^{-1} still fit the P_i release data but suggest a total P_i formation burst of ~25%. $k_{+2} = 75$ s^{-1} and $k_{+3} = 20$ s^{-1} also fit but would give a total P_i formation burst of ~50%. So where $k_{+2} > k_{+3}$, the model would not fit the quenched flow data for total P_i formation burst and k_{-2} would need to be reduced to accommodate oxygen exchange data. $k_{+2} = 22$ s^{-1} and $k_{+3} = 100$ s^{-1} fit our data not quite as well and suggest the total P_i burst is <5%, so this situation cannot be dismissed. It seems probable that $k_{+3} > k_{+2}$ to be most consistent with previous data.

The results presented here show that the kinetics of P_i release can be followed directly using the fluorescent MDCC-PBP probe and the data fit with previous measurements on isolated actomyosin subfragment 1. The data also show the potential for using this technique in fibers where the process of P_i release is likely to be greatly modified by the requirements of force generation.

ACKNOWLEDGMENT

We thank Dr. A. Nakata (Osaka) for providing the original *phoS* clone and Prof. F. Quiocho (Houston) for providing α-carbon coordinates of the PBP structure. We also thank Dr. D. R. Trentham (NIMR, London) for helpful discussions.

REFERENCES

Bagshaw, C. R., & Trentham, D. R. (1973) *Biochem. J. 133*, 323–328.
Banik, U., & Roy, S. (1990) *Biochem. J. 266*, 611–614.
Biosca, J. A., Barman, T., & Travers, F. (1984) *Biochemistry 23*, 2428–2436.
Bowater, R., Zimmerman, R. W., & Webb, M. R. (1990) *J. Biol. Chem. 265*, 171–176.
Bradford, M. M. (1976) *Anal. Biochem. 72*, 248–254.
Corrie, J. E. T. (1990) *J. Chem. Soc. Perkin Trans. 1*, 2151–2152.
Corrie, J. E. T. (1994) *J. Chem. Soc., Perkin Trans. 1* (in press).
De Groot, H., & Noll, T. (1985) *Biochem. J. 229*, 255–260.
Dente, L., Sollazzo, M., Baldari, C., Cesareni, G., & Cortese, R. (1985) in *DNA Cloning*, Vol. I (Glover, D. M., ed.) pp 101–107, IRL Press Ltd., Oxford.
Evans, J. A., & Eisenberg, E. (1989) *Biochemistry 28*, 7741–7747.
Gibson, T. J. (1984) *Studies on the Epstein-Barr virus genome*, Ph.D. Thesis, Cambridge University, Cambridge, England.
Gill, S. C., & von Hippel, P. H. (1989) *Anal. Biochem. 182*, 319–326.
Goldman, Y. E. (1987) *Annu. Rev. Physiol. 49*, 637–654.
Hibberd, M. G., & Trentham, D. R. (1986) *Annu. Rev. Biophys. Biophys. Chem. 15*, 119–161.
Kubena, B. D., Luecke, H., Rosenberg, H., & Quiocho, F. A. (1986) *J. Biol. Chem. 261*, 7995–7996.
Kulikowska, E., Bzowska, A., Wierzchowski, J., & Shugar, D. (1986) *Biochim. Biophys. Acta 874*, 355–363.
Leatherbarrow, R. J. (1992) *Grafit* version 3, Erithacus Software Ltd., Staines, U.K.
Lehrer, S. S., & Kerwar, G. (1972) *Biochemistry 11*, 1211–1217.
Lowry, O. H., & Passonneau, J. V. (1972) *A Flexible System of Enzymatic Analysis*, pp 86–92, Academic Press, New York.
Luecke, H., & Quiocho, F. A. (1990) *Nature 347*, 402–406.

Magota, K., Otsuji, N., Miki, T., Horiuchi, T., Tsunasawa, S., Kondo, J., Sakiyama, F., Amemura, M., Morita, T., Shinagawa, H., & Nakata, A. (1984) *J. Bacteriol. 157*, 909–917.

Mao, B., Pear, M. R., McCammon, J. A., & Quiocho, F. A. (1982) *J. Biol. Chem. 257*, 1131–1133.

Medveczky, N., & Rosenberg, H. (1970) *Biochim. Biophys. Acta 211*, 158–168.

Morita, T., Amemura, M., Makino, K., Shinagawa, H., Magota, K., Otsuji, N., & Nakata, A. (1983) *Eur. J. Biochem. 130*, 427–435.

Nakamaye, K. L., & Eckstein, F. (1986) *Nucleic Acids Res. 14*, 9679–9698.

Rosenfeld, S. S., & Taylor, E. W. (1984) *J. Biol. Chem. 259*, 11908–11919.

Sambrook, J., Fritsch, E. F., & Maniatis, T. (1989) *Molecular cloning. A laboratory manual*, 2nd ed., Cold Spring Harbor Laboratory Press, Cold Spring Harbor, NY.

Sharff, A. J., Rodseth, L. E., Spurlino, J. C., & Quiocho, F. A. (1992) *Biochemistry 31*, 10657–10663.

Shukla, K. K., & Levy, H. M. (1977) *Biochemistry 16*, 132–135.

Sleep, J. A., & Boyer, P. D. (1978) *Biochemistry 17*, 5417–5422.

Sleep, J. A., & Hutton, R. L. (1980) *Biochemistry 19*, 1276–1283.

Stein, L. A., Chock, P. B., & Eisenberg, E. (1984) *Biochemistry 23*, 1555–1563.

Surin, B. P., Jans, D. A., Fimmel, A. L., Shaw, D. C., Cox, G. B., & Rosenberg, H. (1984) *J. Bacteriol. 157*, 772–778.

Taylor, J. W., Ott, J., & Eckstein, F. (1985) *Nucleic Acids Res. 13*, 8765–8785.

Tesi, C., Barman, T., & Travers, F. (1990) *FEBS Lett. 260*, 229–232.

Tesi, C., Kitagishi, K., Travers, F., & Barman, T. (1991) *Biochemistry 30*, 4061–4067.

Trentham, D. R., Bardsley, R. G., Eccleston, J. F., & Weeds, A. G. (1972) *Biochem. J. 126*, 635–644.

Webb, M. R., & Trentham, D. R. (1981) *J. Biol. Chem. 256*, 10910–10916.

Webb, M. R. (1992a) *Proc. Natl. Acad. Sci. U.S.A. 89*, 4884–4887.

Webb, M. R. (1992b) *Philos. Trans. R. Soc. London B 336*, 19–24.

Weeds, A. G., & Taylor, R. S. (1975) *Nature 257*, 54–56.

Willsky, G. R., & Malamy, M. H. (1976) *J. Bacteriol. 127*, 595–609.

Wu, C., Yarbrough, L. R., & Wu, F. Y. (1976) *Biochemistry 15*, 2863–2868.

Yanisch-Perron, C., Vieira, J., & Messing, J. (1985) *Gene 33*, 103–119.